Fabrication and Test of TQS01 – a 90 mm Nb_3Sn Quadrupole Magnet for LARP

S. Caspi, D. Dietderich, P. Ferracin, S.A. Gourlay, A.R. Hafalia, R. Hannaford, A.F. Lietzke, A.D. McInturff, G.L. Sabbi, A. Ghosh ,A N. Andreev, E. Barzi, R. Bossert, V.V. Kashikhin, I. Novitski, G. Whitson and A.V. Zlobin

***Abstract*— In support of the development of a large-aperture Nb_3Sn superconducting quadrupole for the Large Hadron Collider luminosity upgrade, two models (TQS and TQC) with a 90-mm aperture are being constructed at LBNL and FNAL within the framework of the US LHC Accelerator Research Program (LARP). These models use two identical Nb_3Sn coils but have different coil support structures. This paper describes the fabrication, assembly, cool-down and test of TQS01 - a model based on key and bladder technology with supporting iron yoke and an aluminum shell. Comparison of the test measurements with design expectations is also reported.**

***Index Terms*— Superconducting quadrupole, LARP, Nb_3Sn.**

I. Introduction

Three US laboratories (BNL, FNAL, and LBNL) have collaborated in a development program towards the fabrication of a full scale Interaction Region (IR) quadrupole magnet made of Nb_3Sn conductor. The TQ-series magnets are the first R&D step towards an upgrade of the LHC IR and are part of the LHC Accelerator Research Program (LARP) [1]. The defined operational goals (gradient >205 T/m, bore >90 mm, excellent field quality, and high radiation loads) required the use of Nb_3Sn superconducting cable. Using virtually identical coils in two different structures LBNL (magnet TQS01) and FNAL (magnet TQC01) have built and tested two 1m long magnets. The LBNL design is a shell based structure using "key and bladder", successfully tested in a number of different Nb_3Sn magnets [2-7], while the FNAL design is a collar based structure [8-9].

The shell-based structure approach uses bladders for precise, room temperature pre-stress control, with negligible stress "overshoot" during magnet assembly. Interference keys are inserted to retain the pre-stress and allow bladder removal.

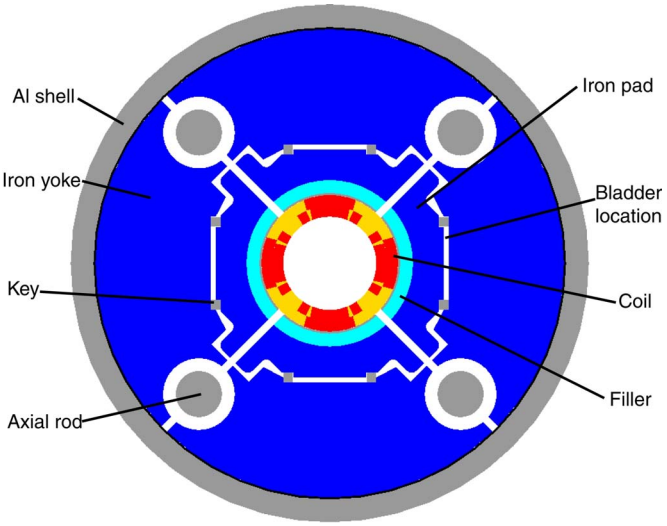

Fig. 1. TQS01 magnet cross-section showing coils, fillers, pads, keys, yokes, skin and axial supporting rods.

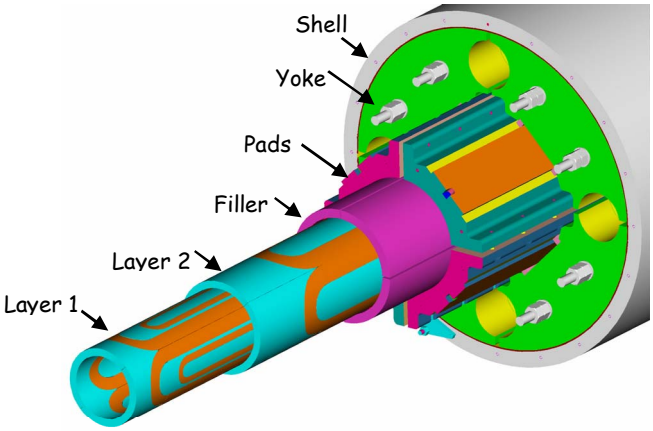

Fig. 2. View of coils and supporting structure

A tensioned aluminum shell compresses internal iron and coil components, and applies a substantial fraction of the operational pre-stress during cool-down. Accordingly, the final coil pre-stress is monotonically approached from below, without overstressing the fragile conductor. A cross-section and assembly are shown in Fig. 1-2.

In section II the structural design and instrumentation is outlined. The assembly and cool-down results are covered in section III. In sections IV through VI the test results and conclusions are discussed.

Manuscript received September 20, 2005. This work was supported by the Director, Office of Energy Research, Office of High Energy and Nuclear Physics, High Energy Physics Division, U. S. Department of Energy, under Contract No. DE-AC02-05CH11231.

First 9 authors are with Lawrence Berkeley National Laboratory, Berkeley, CA 94720 USA (e-mail: s_caspi@lbl.gov).

A. Ghosh is with Brookhaven National Laboratory, NY, USA

Last 7 authors are with Fermi National Laboratory, Batavia, IL, USA

TABLE I
TQS01 MAGNET PARAMETERS

	Unit	Layer 1	Layer 2
STRAND			
Type		MJR	
Diameter	mm	0.7	
Cu/Sc		0.89	
Assumed J_{ss} (4.2 K, 12 T)	A/mm^2	1900	
CABLE			
N strands		27	
Mid-thickness bare	mm	1.26 ± 0.02	
Width bare	mm	10.056 ± 0.05	
Keystone angle	Degree	1.05 ± 0.1	
Insulation thickness	mm	0.125	
COILS			
Turns per block		6/12	16
Mandrel diameter	mm	90	
STRUCTURE			
Shell thickness	mm	22	
Shell outer diameter	mm	500	
OPERATING EXPECTATIONS at 4.4 K (1.9 K):			
Short sample current	kA	12.1	
Peak conductor field	T	10.9	9.68
G_{ss}	T/m	216	
Stored energy	kJ/m	370	
Inductance	mH/m	5	
Coil Lorentz mid-plane stress	MPa	123	83
Fx per quadrant	MN/m	2.8	
Total Lorentz axial end force	kN	331	

TABLE II
TQS01 STRESS-STRAIN - CALCULATIONS

	STRESS (MPa)		STRAIN (με)	
	300K	4.4K	300K	4.4K
Shell azimuthal	29	180	373	1510
Shell axial Z	4	149	0	1236
Rods axial Z	9	177	-16	1473
Island azimuthal	-62	-274	-443	-2318
Island axial Z	-44	14	-230	807
Turn 1 (pole)	-43	-163		
Turn 1 (pole) z	-26	-12		

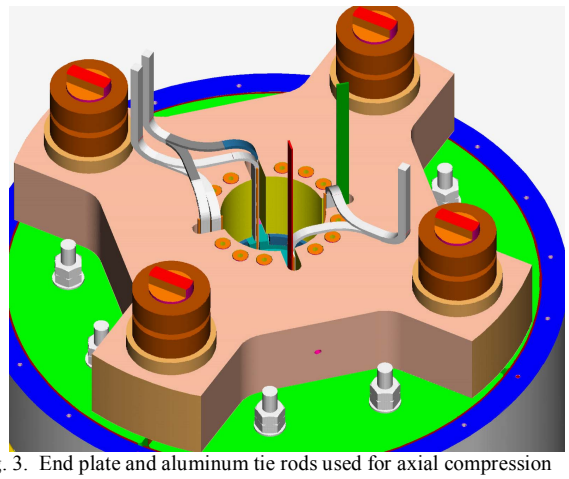

Fig. 3. End plate and aluminum tie rods used for axial compression

II. MAGNET DESIGN AND INSTRUMENTATION

A. Conceptual design and parameters

The magnet design was fully integrated with analysis. The analysis was done in 3D using three major programs: ProE (CAD), TOSCA (magnetic analysis), and ANSYS (structural analysis). Friction factors were between $\mu = 0.2$ and 0.6. The results from the combined analyses provided 1) the target room-temperature azimuthal and axial assembly pre-stress, predicted 2) the cool-down impact on pre-stress and 3) provided axial and azimuthal response during excitation. The specs for the magnet stress at 4.5 K were set to prevent any possible coil-island separation in the straight section and the ends. One of the more distinct differences between TQS01 and the TQC01 was the way pre-stress was applied and the magnitude of axial pre-stress. Based on extensive ANSYS studies 800 kN (at 4.4 K) of axial force was needed to prevent coil-island separation in the ends and overcome frictional forces between the coils and the surrounding structure. This was accomplished by four aluminum tie-rods pulling end plates against the ends of the coils at cool down (Fig. 3). Only 35% of that force is actually applied during assembly the rest builds up during cool-down by the contracting axial aluminum tie rods. To overcome frictional forces the applied axial force had to be more than twice the maximum Lorentz force. To reduce the influence of friction, pre-stress during assembly was first applied axially (by a hydraulic cylinder) and then azimuthally (by bladders). A cool-down test at 77 K determined the friction factor between the yoke and the shell to be 0.6. Between all other components a friction factor of 0.2 was used in the analysis.

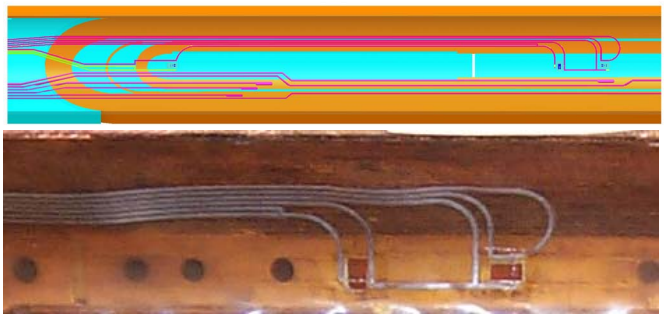

Fig. 4. Strain gauges near the magnet center and lead-end (top), the gap between island sections and center gauges (bottom).

Design parameters and calculated pre-stress are shown in Tables I and II. Strain gauges were used to measure and verify the calculated values.

B. Strain gauges

In a collaborative effort 14 coils were wound and cured at FNAL and reacted and potted at LBNL (8 for TQS and TQC, 2 spares and 4 spares). The TQS01 coils were instrumented with voltage taps and strain gauges glued to layer 1 island (Fig. 4). Two half bridges were located on the island center to measure azimuthal and axial strain and an additional axial gauge was placed near the lead end. The gauges where thermally compensated by gauges mounted on stress-free elements. Fully compensated strain gauges were also used on the shell and the axial tie rods. Measured strain in two principal directions (and assuming no shear)

was converted into stress using the following relationships and properties of bronze (islands) and aluminum (shell):

$$\sigma_\theta = \frac{E}{(1-\nu^2)}(\varepsilon_\theta + \nu\varepsilon_z) \quad \sigma_z = \frac{E}{(1-\nu^2)}(\varepsilon_z + \nu\varepsilon_\theta).$$

III. Assembly and Cool-down

The magnet was assembled from two subassemblies [10]: a coil pack of four coils held together by four adjustable load pads to ensure uniformity. A structure pack of four iron yokes separated temporarily by gap-keys and held by an outer aluminum shell. During final assembly the gap-keys were removed and interference keys inserted between pads and yokes using pressurized bladders. The coils were pre-stressed azimuthally and axially. While holding the coils snuggly within the structure, an axial end force was applied (using a piston) to the coils ends by tensioning four tie-rods to 37 MPa. Azimuthal pre-stress was then applied using keys and bladders. The final coils pre-stress was -43 MPa azimuthally and -26 MPa axially (Table II).

The operational pre-stress was reached during cool-down. Differences in the thermal contraction properties between aluminum and iron continued to increase pre-compression in the coils. At 4.4 K the measured shell tensile stress increased to 150 MPa azimuthally and 140 MPa axially and the rod axial stress increased to 110 MPa. Measured stresses in the coil islands were -180 MPa azimuthally (compression) and 25 MPa axially (tension), partially confirming ANSYS calculations regarding property differences and friction factors between the coil and its supporting structure.

IV. Test Results

A. Quench Performance

The magnet first quench was at 80% of short sample (176 T/m) and trained to 190 T/m (Fig. 5) in a dozen quenches. Most quenches started in a single coil (#6) and at the same location in layer 1 straight section near the layer 1 to layer 2 ramp. None of the quenches (except one) started in the ends (the field on the conductor is the same in the straight section and the end). Additional test results can be found in [11].

B. Measured strain

Measured strain-stress from cool-down to warm-up is shown in Figures 6-7. At 75% of the Lorentz force the island compressive azimuthal stress was reduced to -30 MPa (a decrease of 150 MPa) and at the same time the island tensile axial stress increased from 30 MPa to almost 90 MPa. The overall strain results were within expectations; however future refinement to the ANSYS model may be required by revising friction coefficients. Fig. 8 shows measured changes of stress in the island during excitation. Small changes in stress over several quenches are evidenced by "ratcheting".

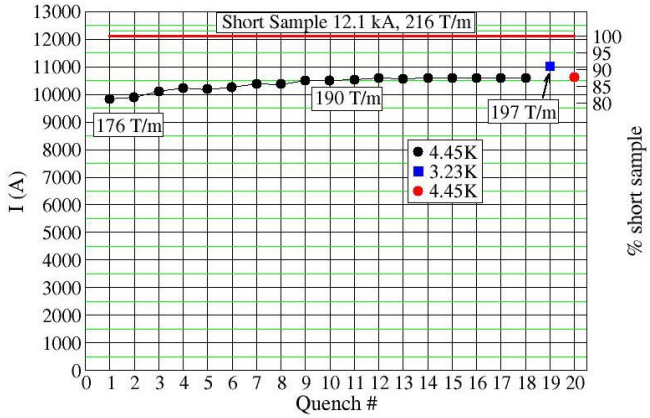

Fig. 5. Magnet training and expected "short-sample".

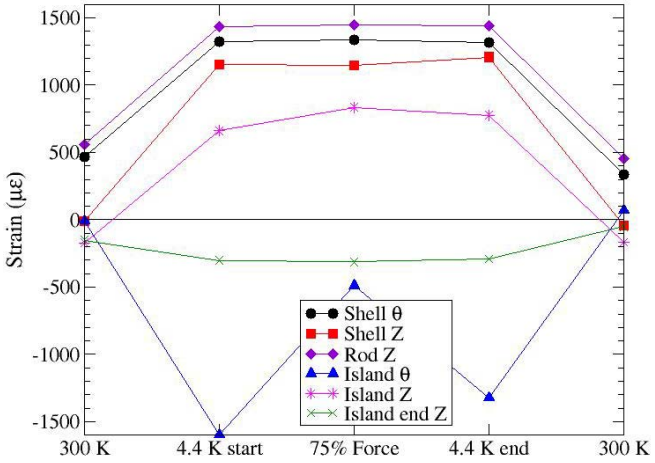

Fig. 6. Measured strain from cool-down to warm up.

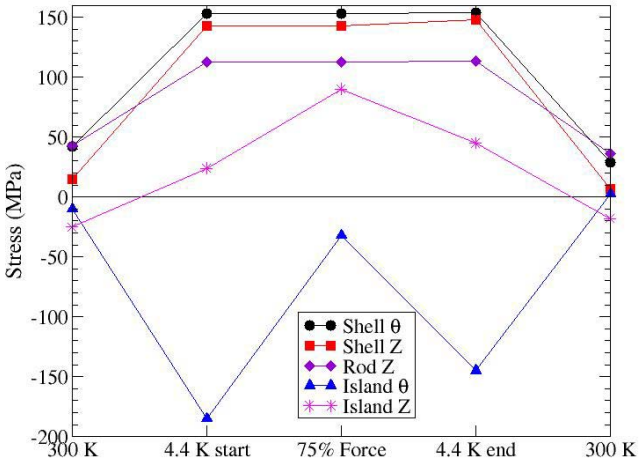

Fig. 7. Measured stress from cool-down to warm up

V. Post Analysis

A. Island gaps

A post-test visual inspection of the fiberglass-reinforced epoxy in the gap between island sections revealed discoloring or "crazing" - typical of high tension. A post structural analysis, that included island sectional gaps, showed a significant increase in axial tensile stress especially in the conductor turn near the gap. Plots of the axial stress along the coil-island interface are shown in

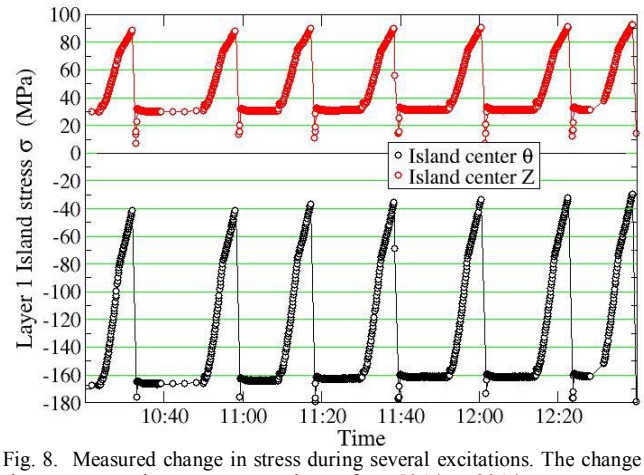

Fig. 8. Measured change in stress during several excitations. The change in slope corresponds to a ramp rate change from 50A/s to 20A/s.

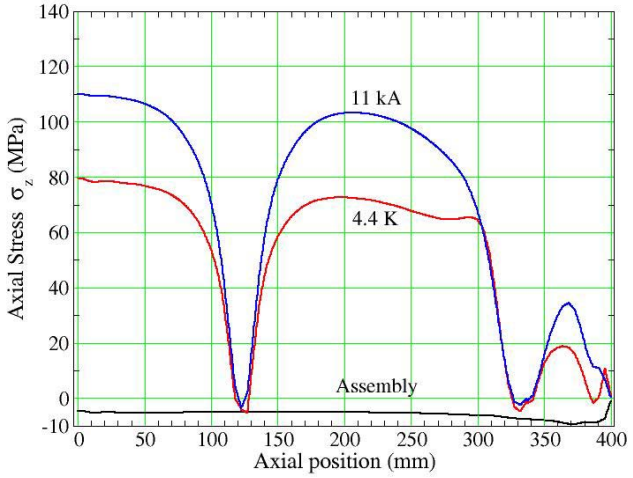

Fig. 9. Calculated axial stress showing a dips in the island gaps.

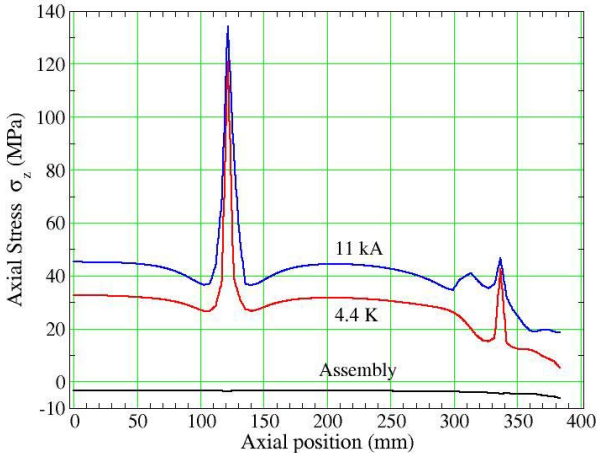

Fig. 10. Calculated axial stress in turn 1 near the island peaking across the island gaps.

Figures 9-10 (with zero at the magnet center and moving to its end).

The tensile axial stress in the island near the magnet center increases with cool-down and excitations, but tends to decrease towards the magnet end. The coil axial stress (turn 1 around the island) more then doubles near the center island gap (at 125 mm). The localized high tensile strain in the coil near the island gap may why the magnet did not reach its expected short sample. The increase in tensile stress of the coil correlates well with the lower thermal expansion of the iron yoke. Friction between the coil and the yoke prevents the coil from contracting axially thus placing the coil in tensile stress. The island, acting as a structural rib within the coil, protects the coil as long as its interface with the coil can sustain axial tensile shear. One way to reduce tension in the island and prevent conductor strain at the gaps is to replace the bronze-islands with titanium-islands. Analysis confirms that with Ti islands, the island-gaps remain closed even after cool-down and the coil remains protected.

VI. Conclusions

Design and test results of TQS01 are presented. The magnet started training at 80% of short sample and achieved 87% in a dozen quenches. Most quench locations were confined to a local spot in coil #6 near the gap in the pole. Except for one occurrence there were no quenches in the magnet ends. A high axial tensile stress was measured in the island in agreement with analysis. We assume that axial stress in the coil near the gaps was the main reason for the 13% reduction in current. Replacing the bronze islands with titanium should improve magnet performance.

Acknowledgments

We thank our technical staff for their hard work and dedication.

References

[1] LARP website, http://www.agsrhichome.bnl.gov/LARP/.
[2] G. Sabbi *et al.*, "Nb3Sn quadrupole magnets for the LHC IR", *IEEE Trans. Appl. Superconduct.*, Vol. 13, no. 2, June 2003, pp. 1262-1265.
[3] S. Caspi, *et al.*, "Mechanical design of a second generation LHC IR quadrupole", *IEEE Trans. Appl. Superconduct.*, Vol. 14, no. 2, June 2004, pp. 235-238.
[4] S. Caspi, *et al.*, "The use of pressurized bladders for stress control of superconducting magnets", *IEEE Trans. Appl. Superconduct.*, Vol. 11, no. 1, March 2001, pp. 2272-2275.
[5] A. R. Hafalia, *et al.*, "A new support structure for high field magnet", *IEEE Trans. Appl. Superconduct.*, Vol. 12, no. 1, March 2002, pp. 47-50.
[6] A. R. Hafalia, *et al.*, "Structure for an LHC 90 mm Nb_3Sn quadrupole magnet", *IEEE Trans. Appl. Superconduct.*, Vol. 15, no. 2, June 2005, pp. 1444-1447.
[7] P. Ferracin, *et al.*, "Assembly and test of SQ01b, a Nb_3Sn quadrupole magnet for the LHC Accelerator Research Program", *IEEE Trans. Appl. Superconduct.*, vol. 16, no. 2, June 2006, pp. 382-385.
[8] R.C Bossert, *et al.*, "Development of TQC01, a 90 mm Nb_3 Sn model quadrupole for the LHC upgrade based on SS collars", IEEE Trans. Appl. Superconduct., vol. 16, no. 2, June 2006, pp. 370-373.
[9] R.C. Bossert, *et al.*, "Development of LARP Technological Quadrupole (TQC) Magnets" paper 1LK02 this conference.
[10] S. Caspi, *et al.*, "Design and analysis of TQS01, a 90 mm Nb_3 Sn model quadrupole for the LHC luminosity upgrade based on a key and bladder assembly", *IEEE Trans. Appl. Superconduct.*, vol. 16, no. 2, June 2006, pp. 358-361.
[11] A.F. Lietzke, *et al.*, "Analysis of Test Results for TQS01, a High-Field Nb3Sn Quadrupole for LARP" paper 1LK03 this conference.